Highly efficient bidirectional Silicon Carbide power converter for Electric Vehicle flywheel emulator

Alexandre de Bernardinis, Richard Lallemand, Abdelfatah Kolli

Highly efficient bidirectional Silicon Carbide power converter for Electric Vehicle flywheel emulator

Alexandre De Bernardinis*
Department of Industrial Maintenance Engineering – LMOPS (UR4423)
IUT de Thionville-Yutz
University of Lorraine, Yutz, France
e–mail: alexandre.de-bernardinis@univ-lorraine.fr

Richard Lallemand, Abdelfatah Kolli
SATIE
University Gustave Eiffel, Versailles, France
e–mail: richard.lallemand@univ-eiffel.fr
e–mail: abdelfatah.kolli@Gmail.com

ABSTRACT

Flywheels are nowadays a solution for the dynamic charging of electric vehicles since they act as transient energy storage. The need of a top efficient reversible power converter for the flywheel system is crucial to assure high dynamic performance. The paper presents the design of a 50kW highly efficient bidirectional three-phase DC-AC inverter involving most recent Silicon carbide metal oxide semiconductor field effect transistors and its experimental validation on home-made emulator. Highest efficiency in reversible mode, compactness and thermal enhancement are the target objectives that have been achieved. The converter prototype is evaluated on an original Pulse Width Modulation testing-bench able to emulate the working of the flywheel system. High frequency Pulse Width Modulation switching, speed cycle operating and thermal losses are evaluated. Also an efficiency above 99% for the converter has been attained, enabling a robust functioning of the flywheel system emulator able to perform specific charging profiles.

KEYWORDS

DC/AC Converter; Electric Vehicle; Flywheel; MOS Field Effect Transistor; Pulse Width Modulation; Silicon carbide.

INTRODUCTION

Among recent developments in energy storage techniques cited by [1], Flywheel Energy Storage System (FESS) is an electromechanical energy storage system which can exchange electrical power with the electric network [2]. It consists in an electrical machine, DC-AC converter, DC link capacitor and a massive (steel or composite materials) disk. Unlike other storage systems such as the Battery Energy Storage System (BESS), FESS is an environmentally-friendly short- or medium-term energy storage system, which has the capability of numerous charge and discharge cycles. These characteristics make the FESS a suitable choice for different applications in the power system such as power quality improvement, power smoothing, renewable energies integration support, stability improvement, etc. Flywheel Energy Storage System (FESS) can hence be applied in various domains, from very small micro-satellites to huge power networks as reported by [3]. Energy

* Corresponding author

storage systems (ESS) with ultra-long lifetime of over twenty years using matrix converters and flywheels to compensate frequency and voltage fluctuations for the power grid are solutions to be considered [4, 5]. Flywheels have the advantage of providing maintenance-free for over twenty years.

Also flywheels sometimes involve the use of superconductor materials dedicated for high speed devices as stated in [6], and behave as dynamic energy storage systems for residential microgrids and for power management in electric vehicles (EVs) as recovering the braking energy [7, 8], for the control and stability of the grid voltage involving specific control laws and strategies. There are three main devices composing a FESS, including the AC machine as Permanent Magnet Synchronous Motor (PMSM), bearing, and power electronics interface which technology can be based on Silicon carbide (SiC) devices, alike SiC MOSFETs, or JFET body diodes [9] for attaining highest efficiency, compactness and thermal enhancement.

The manuscript is a post *IEEE ITEC 2017* contribution for which a first approach of the work has already been published by authors [20]. The present manuscript focuses on a progress of the previously published work, including novel achieved results in particular, the calculation of the electro thermal highest efficiency of the SiC power inverter for usage profiles, and the dynamic evaluation of the converter on a homemade emulator that reproduces in laboratory the technological behavior of a flywheel energy storage system (FESS) dedicated to electric vehicle recharging.

The purpose of this paper is to propose the concept and realization of an originally-designed bidirectional 50kW three-phase DC-AC inverter with novel Silicon carbide (SiC)-based MOSFETs transistors technology used for the power supply of a flywheel energy storage system dedicated to electric vehicles charging.

The research work, which is mainly experimental, provides real technological innovation, in both designs the power converter itself and the hardware emulator since they utilize the most recent wide band-gap silicon carbide semiconductors, and original robust control strategy.

The work is carried-out in the framework of the French “VIVE” project supported by the French ministry of Industry and Region of Paris-Île de France. Highest efficiency in reversible mode, compactness and thermal enhancement are the target objectives and research highlights for the converter prototype. The three-phase DC-AC Silicon carbide inverter prototype is tested on an original home-made PWM test-bench which semiconductor switches are controlled using the modulated hysteresis controller and which is able to emulate the working of the PMSM - flywheel system. High frequency PWM tests, design aspects for the DC busbar, speed cycle operating and thermal losses are evaluated. Adopted design for realization and control strategy should permit to reach the highest efficiency for the DC-AC inverter.

The paper is organized as follows: In section II a recent literature overview is proposed on Flywheel energy storage systems and Silicon carbide converters used as power electronics supply for FESS. Section III focuses on the SiC-based DC-AC inverter design for EV-charging Flywheel system. Section IV presents experimental pulse width modulated (PWM) switching tests, interface driver card design for the SiC MOSFETs switches and DC Bus hardware design. Section V deals about the experimental validation for the SiC DC-AC inverter implemented on the original, and modular, double-converter PWM test bench controlled using the modulated hysteresis method. Finally section V ends with the evaluation of static, then speed cycle thermal losses and calculation of SiC DC-AC inverter efficiency.

II. LITERATURE SURVEY

This section describes a literature overview on Flywheel Energy Storage Systems (FESS) and Silicon carbide power converters. It starts with power electronics topologies feeding FESS, and

then enumerates any applications of the Flywheel technology as energy storage device in several domains. Examples of research works and realizations is this field are given hereafter.

A bidirectional converter (BDC) is essential in applications where energy storage devices are involved. Such applications include transportation, battery less uninterruptible power system, flywheel energy storage systems, etc. Bidirectional power flow through buck and boost modes of operation along with high power density and efficiency is an important requirement of such systems. A novel BDC topology using a combination of fast turn-off Silicon controlled rectifier (SCR) and Insulated-gate bipolar transistor (IGBT) with a novel control logic implementation to achieve zero switching losses through zero voltage transition and zero current transition techniques has been designed by [10]. According to [11], Flywheel energy storage systems (FESS) can be used to store and release energy in high power pulsed systems. Based on the use of a homopolar synchronous machine driving a FESS, a high performance model-based power flow control law has been developed by S.J. Amodeo et al. using the feedback linearization methodology. To reduce the magnetic losses, a pulse amplitude modulation driver for the armature is more adequate. The restrictions in amplitude and phase imposed by the driver are also included. A full order Luenberger observer for the torque angle and rotor speed is developed to implement a sensorless control strategy. In [12] a novel flywheel energy storage system is proposed which results in up to 20% enhancement in the harvested energy from the flywheel, in comparison with the existing systems. Generally, boost converters are used for boosting the voltage in such systems. Major limitation of a boost converter is the dependency of its maximum achievable voltage gain on the ratio of its source resistance to load resistance which limits the amount of harvested energy from a flywheel and lowers the efficiency at low input voltages. In [13] Koos van Berkel et al. state that mechanical hybrid powertrains have the potential to improve the fuel economy of passenger vehicles at a relatively low cost, by adding a flywheel and only mechanical transmission components to a conventional powertrain. This paper presents a systematic approach to optimizing the topology and flywheel size, which are the key design parameters of a mechanical hybrid powertrain. The topology is optimized from a limited set of over twenty existing mechanical hybrid powertrains described in the literature. After a systematic classification of the topologies, a set of four competitive powertrains is selected for further investigation. The fuel-saving potential of each hybrid powertrain is computed using an optimal energy controller and modular component models, for various flywheel sizes and for three certified driving cycles. The hybridization cost is estimated based on the type and size of the components. Other criteria, such as control complexity, clutch wear, and driving comfort are qualitatively evaluated to put the fuel-saving potential and the hybridization cost into a wider perspective. Results show that, for each of the four investigated hybrid powertrains, the fuel-saving benefit returns the hybridization investment well within (about 50%) the service life of passenger vehicles. The optimal topology follows from a discussion that considers all the optimization criteria. The associated optimal flywheel size has an energy storage capacity that is approximately equivalent to the kinetic energy of the vehicle during urban driving (50 km/h). Fast charging stations (FCS) are able to recharge plug-in hybrid electric vehicles (pHEVs) in less than half an hour, thus representing an appealing concept to vehicle owners since the off-road time is similar as for refueling at conventional public gas stations [14]. However, since these FCS plugs have power ratings of up to 100 kW, they may expose the utility mains to intolerable stresses in the near future scenario where there will be a large number of public FCS spread across the network. Authors of paper [14] proposes a comprehensive review of DC Fast-Charging Stations with Energy Storage: Architectures, Power Converters, and Analysis. In [15] authors proposes a control strategy for plug-in electric vehicle (PEV) fast charging station (FCS) equipped with a flywheel energy storage system (FESS). The main role of the FESS is not to compromise the predefined charging profile of the PEV battery during the provision of a hysteresis-type active power ancillary service to the overhead power system. In that sense, when

the active power is not being extracted from the grid, an FESS provides the power required to sustain the continuous charging process of the PEV battery. A key characteristic of the whole control system is that it is able to work without any digital communication between the grid-tied and FESS converters. The presented experimental results have proved the high accuracy of the theoretical analysis.

In [16] Silicon (Si) carbide (SiC)-based power switching devices provide significant performance improvements compared to conventional Si devices. The superior characteristics enable considerable loss, size, and weight reduction of power converters in the powertrain of hybrid/electric vehicles. However, the fast switching capability of SiC devices renders them more vulnerable to parasitic inductances in the circuit. Hence, the impact of interconnection inductances to overvoltage during turn-OFF transient of SiC devices should be taken into account.

III. SILICON CARBIDE DC-AC INVERTER FOR EV FLYWHEEL CHARGING SYSTEM

As stated in Section II in the review, Flywheels energy storage systems (FESS) are also nowadays becoming more and more potential candidates for utilization as hybrid-storage sources in association with batteries within electric cars. As an example, the active electromagnetic slip coupling kinetic energy recovery system is potentially a cost-effective, yet efficient method for energy transfer between a vehicle and a lightweight flywheel, presented by [17]. According to the authors, the proposed kinetic energy recovery system (KERS) may be less costly and less complex than flywheel-batteries as it needs only one electrical machine and one power electronic converter. Moreover, the storage system is capable of recovering much more mechanical power than its electrical ratings. Furthermore, since a great part of the energy exchange takes place in mechanical form, only a fraction of the captured energy needs to be processed by the power electronic converter. Also, the research described in [18] is aimed at exploring the effect of a dual-mass flywheel on the torsional vibration characteristics of a power-split hybrid powertrain. Other recent research works presented by authors themselves concern two front wheel-motor drives [19], the dynamic recharging of electric vehicles, or for their use as reversible dynamic power sources for EV recharging stations. The work presented in this paper is part of the French VIVE project (VIVE: “Volant d’Inertie pour Véhicules Electrifiés”) coordinated by AER-Atmostat Company, with the supports of the French ministry of Industry and Region of Paris-Île de France in the framework of the FUI (Fonds Unique Interministériel) grant agreement, which objective is to realize, characterize, and implement a flywheel system from AER-Atmostat for EV-charging [20]. From the general powertrain shown in Fig. 1, the presented study concerns the three-phase interface DC-AC inverter (in dashed red lines in Fig. 1), connected to the variable DC bus (580V up to 620V) and supplying the 60kW-Neodymium Iron Boron Permanent magnet synchronous motor (PMSM), 8 poles, whose frequency of the fundamental voltage varies in the range of 100 Hz to 400 Hz depending on the rotor mechanical speed (3.000 to 6.000 rpm).

The Flywheel system with its PMSM motor/generator, and interface inverter is connected through the DC bus to a 3-phase reversible converter ensuring current reinjection/supply with the 380V/ 50Hz grid network and connected to a mixed DC-AC 3-phase plant for EV-dynamic recharging. A 2-level control strategy is used for the powertrain control. Level 1 deals with supervision, security issues, having as inputs the different use-case scenarios (named as macroscopic level). Level 0 (close-up control level) includes the control strategy in (d,q) Park reference frame for the three-phase PMSM currents and provides through a Real-Time prototyping system the PWM signals to the gates of the 3-phase DC-AC inverter transistors. DC voltage security limit up to V_{DCmax} = 700V is added for the inverter protection.

In the FESS a three-phase resistive bloc (named security resistors) has been added at the input stage of the motor-flywheel system (Fig. 1), enabling the flywheel energy discharge in case of emergency situation, in twelve minutes approximately.
For designing the DC-AC inverter prototype and meet the research objectives, Silicon carbide (SiC) MOSFETs in a 1200V/300A Half-Bridge configuration have been chosen from the newest market technology. The goal is to have a high efficiency, compactness and thermal performance for the DC-AC power converter solution, in order to meet industrial challenges for the civil implementation of the EV-charging Flywheel energy storage system. The objective is to reach the highest efficiency in both reversible energy flows for the 60 kW Flywheel/PMSM/inverter system. For switching constraints, up to 100 kHz (max) driver card have been used.

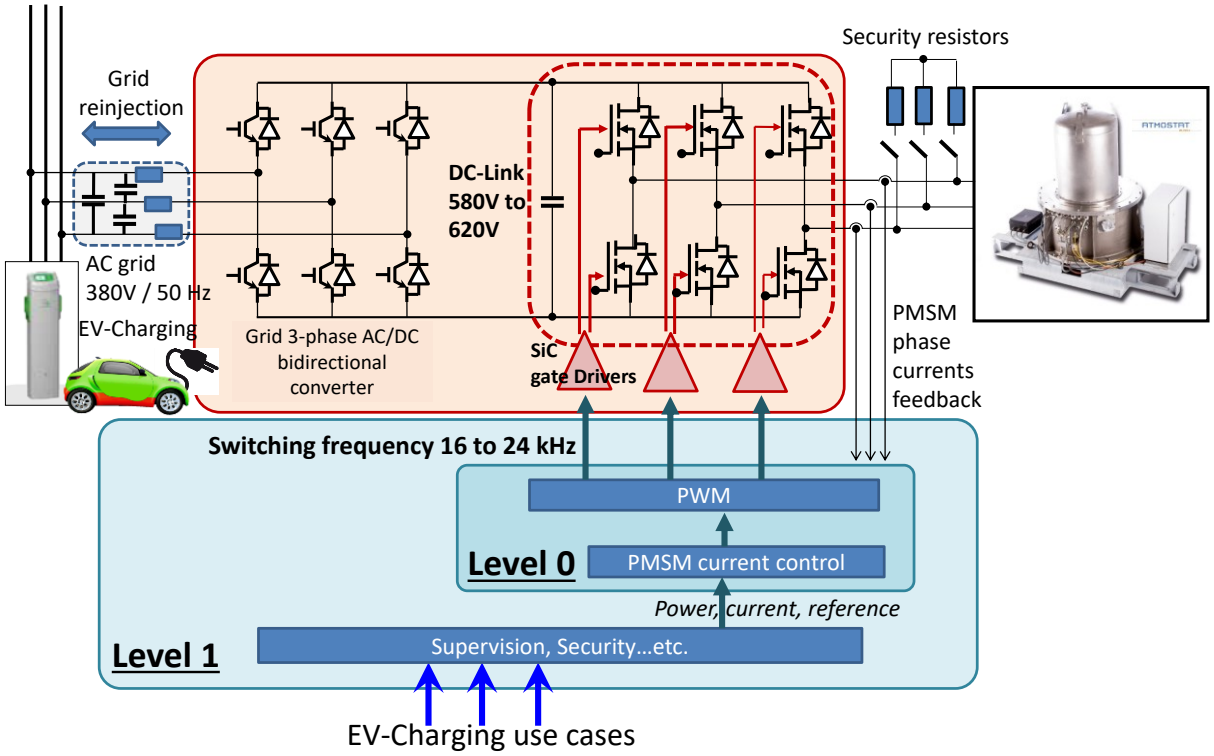

Figure 1. General overview of the FESS (Flywheel Energy Storage System) used for EV-charging

Figure 2 illustrates the high speed deep deflux operation 60kW PMSM from Phase Motion control S.p.A power profile (Watt) vs. speed (rpm). The objective is to operate at constant power over the maximal speed range, with, however, a current limitation up to 144 Arms (203 Amax). At low speed, hence for low motor back-emf (electro-motive force) voltage, active power is linearly limited for 50kW and 60kW.
First switching tests have been performed on a SiC Half-bridge leg and are reported in Section 4. Figure 3 depicts the laboratory experimental set-up for the switching tests of the 1200V/300A Half-Bridge with its high speed driver card connected to the gates. Initial tests have already been performed in the range of 16 to 20 kHz. The switching frequency is increased up to 24 kHz for the thermal losses evaluation and DC-AC converter efficiency calculation. Snubber capacitor has been added in order to minimize the voltage overshoot and oscillations during switching times.

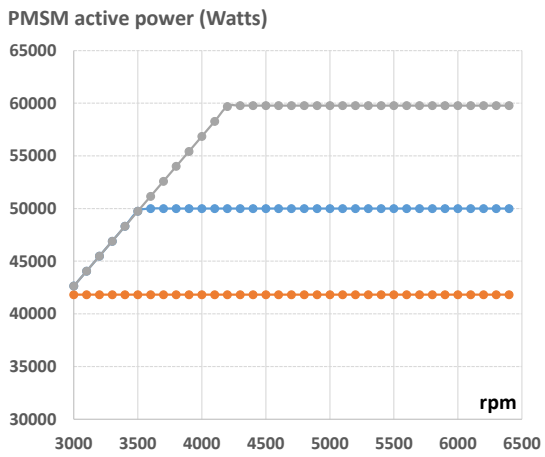

Figure 2. PMSM power profile with current limitation

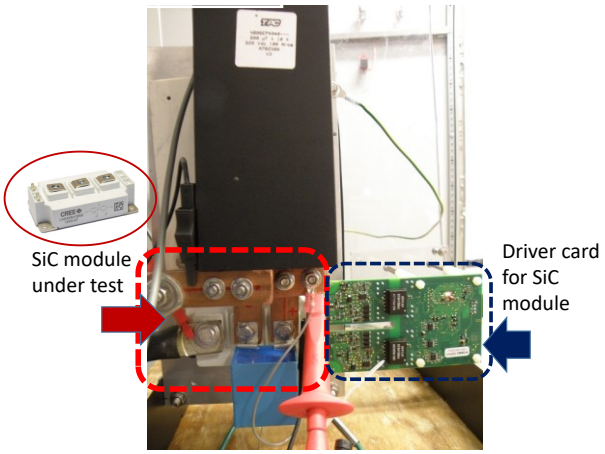

Figure 3. Fig. 3: Experimental set-up for HF switching test of the SiC 1200V/300A Half-Bridge with driver card

Figure 4 shows a comparison of the module efficiency between classical IGBT Silicon technology from SEMIKRON© and Silicon carbide MOSFETs from CREE® (Wolfspeed© Group) for the same component caliber and PMSM power values. Efficiencies have been calculated analytically using the manufacturer's datasheets of the semiconductors. A gain of 5 points (5%) is obtained for the same power constraint (at 60 kW) using the Silicon carbide technology.

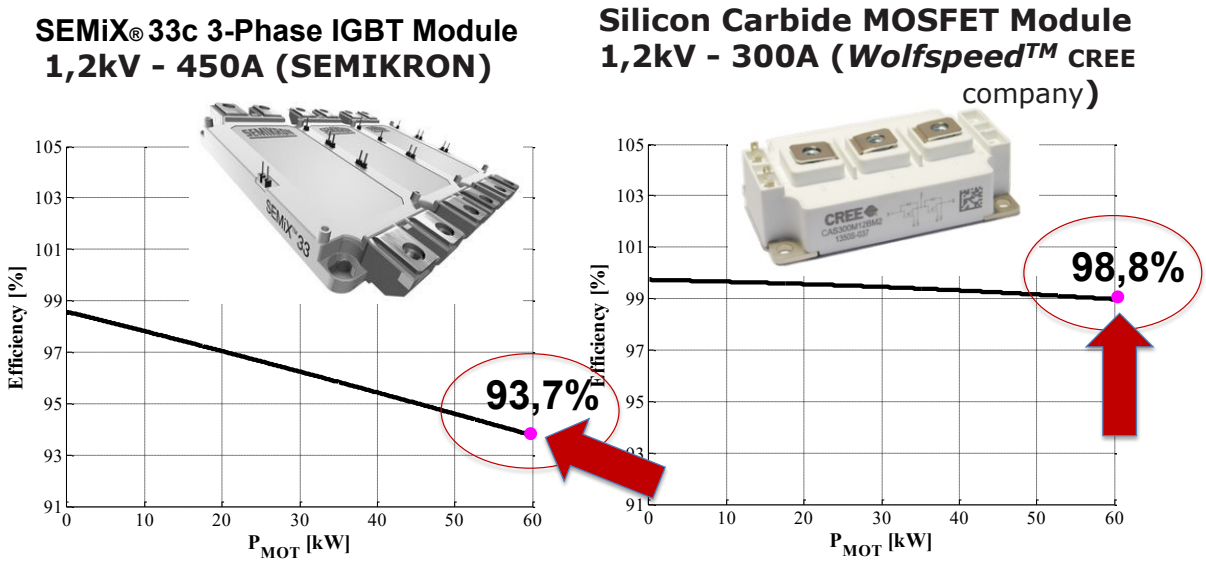

Figure 4. Comparison of the efficiencies for Silicon and Silicon carbide (SiC) semiconductor modules according to motor system's power (kW)

IV. PWM SWITCHING CHARACTERISTICS AND TESTS

The layout of the paper should follow the style of this document, starting with a title, name(s) of author(s) and affiliation(s).

4.1. Experimental switching tests for the SiC MOSFETs

Figures 5a) and 5b) respectively present the switching ON (a) and OFF (b) waveforms for 20kHz frequency performed on the SiC MOSFETs devices. Oscillations amplitude phenomena, in particular for turn-off, have been attenuated using a 2µF snubber capacitor connected in parallel to the MOSFETs Half-Bridge. Turn-On time is 300ns, turn-off about 400ns. Losses and efficiency for the DC-AC inverter will be given in Section 5.3. Numerical acquisitions have been done using oscilloscope Lecroy Wave runner HRO64i, the Vds measurement with sensor PM9100, Ids measure using shunt LEM25 10mΩ, and Vgate with Tektro P5050 recorder.
Laboratory experimental test bench equipment permits to reproduce high frequency PWM control signals applied to the SiC MOSFET Half-Bridge. Figure 7 shows PWM gate control signals, and focus on the AC-phase current. Picture denotes that the current is accurately controlled without any disturbances.

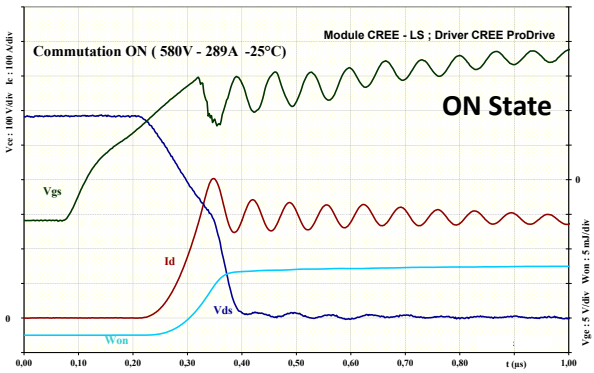

Figure 5.a) SiC MOSFET switching ON state

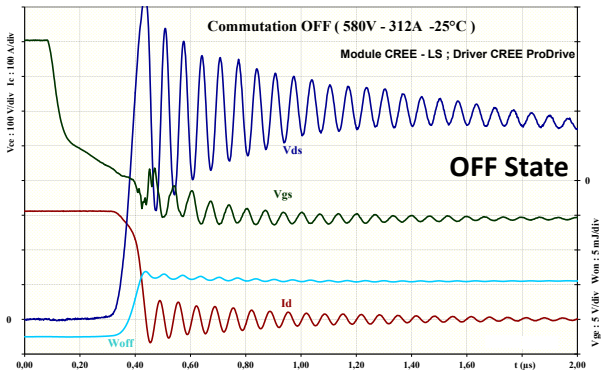

Figure 5.b) SiC MOSFET switching OFF state

4.2. Interface driver card design

The driver card is composed of two input (0 to 5V) PWM (Pulse width modulation) stages corresponding to the upper and lower MOSFETs of the half-bridge. Each stage has an optocoupler HCPL-3120 for the isolation and voltage conditioning of the input voltage signal. Then the signal is boosted using the Traco© Power supply, to the input of the CREE Prodrive© technologies card PT62SCMD12. The driver interface synopsis for one SiC inverter leg is given in Fig. 6a.

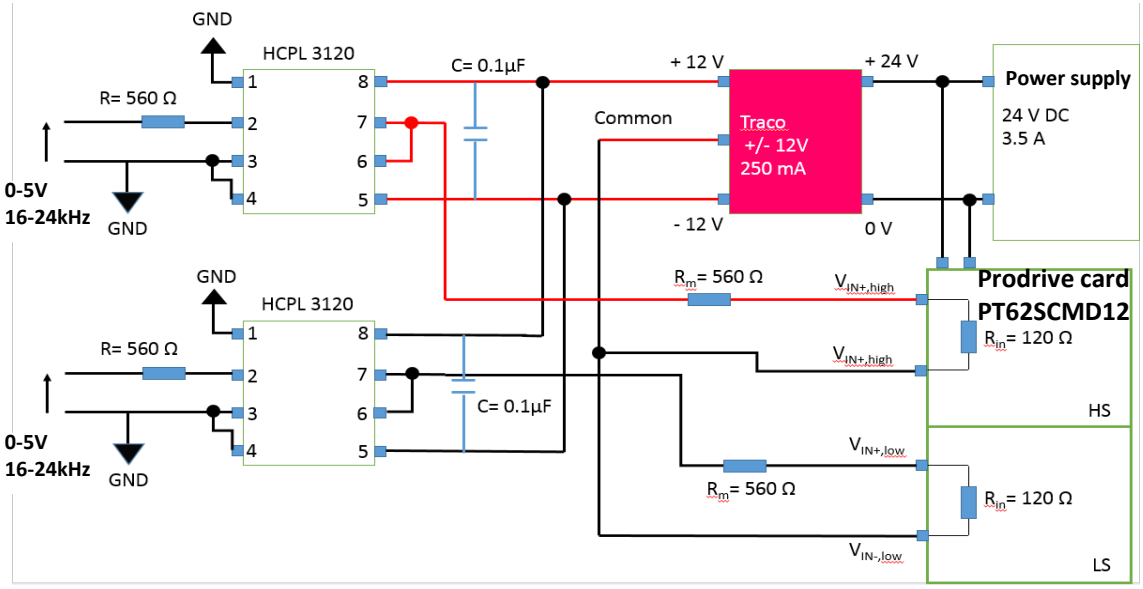

Figure 6.a) Driver interface synopsis with HCPL-3120 optocoupler for one SiC inverter leg

First, to be operated, the OCP (Over Current Protection) mode of the driver card should be deactivated, then the driver card is supplied in 24VDC and the waveforms are acquired on the digital Yokogawa© high speed scope recorder. The yellow waveform in Fig. 6b) represents the control signal injected in the HCPL-3120 optocouplers, the green curve represents the input voltage of the LS (Low side) driver card and is between 1.5 V and -2 V. The purple curve is the HS (High side) part of the driver (2 V). Finally the red waveform highlights the MOSFET voltage of the LS part of SiC module, it should be noted we obtain +20V for the ON state and -6 V for the OFF state. We should however notice that there appears a phase-shift between the input of the driver card and the output gate control signal of LS MOSFET. The measured delay is Toff_fall= 250 ns, the manufacturer's data of the driver card estimates the Toff_fall between 250 and 300 ns, hence there is a good concordance. We also measured the Toff_rise = 610 ns. The manufacturer's data gives a Toff_rise between 400 and 500 ns. We have hence validated the switching operating of a SiC Half-bridge and have realized the complete interface card design for the 3 legs.

Figure 6.b) Driver card Prodrive® gate output Switching results up to 100 kHz

Using the ProDrive® driver cards, in Fig. 7 a focus is given for a 20 kHz PWM gate signal and AC phase current (view on Yokogawa® Digital scope recorder).
Fig. 8 illustrates the realized DC-AC SiC Inverter prototype (with current LEM© sensors and driver cards ProDrive®) designed and built at the SATIE laboratory.

V. EXPERIMENTAL VALIDATION

5.1 Original reversible PWM double-converter tester for hardware emulator

The proposed hardware emulator architecture is original, it has been completely home-made designed in the laboratory. It is composed of two bi-directional converter, the "tester" composed of 3 IGBT/Diode Silicon PWM half-bridges based on Infineon semiconductor technology EconoDUALTM FF450R12ME3 (1200V, 450A) with trench/fieldstop IGBT3 and emitter controlled high efficiency diode (Right side in Fig. 11), and the SiC CREE® CAS300M12BM2 (1200V, 300A) DC-AC PWM inverter under test (DUT) (Left side in Fig. 9).

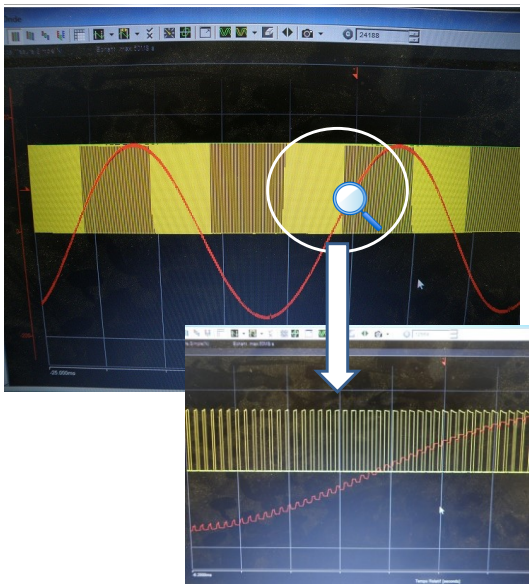

Figure 7. Focus on 20kHz PWM gate signal and AC phase current (view on digital scope recorder)

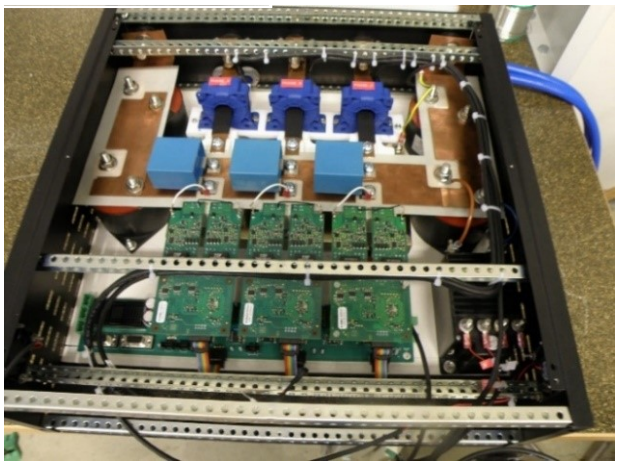

Figure 8. DC-AC Inverter prototype on heatsink (with DC busbar, current LEM© sensors, capacitor's snubber and interface driver cards for CREE ProDrive®). The DC-AC inverter is water cooled

Both inverters are linked with three high frequency filtering (L=1mH) inductances from SMP Company, and powered by a 600 VDC power supply. The "tester" emulates the behavior of the motor/flywheel system. It authorizes $200A_{max}$ in the DC side, and $500A_{p-p}$ in sinusoidal current waveform and up to 500 Hz fundamental frequency. The switching frequency ranges from 0 up to 50 kHz. The strategy integrates current control (Ia, Ib, Ic), thermal (thermistor) and voltage protection (V_{DClim}= 700VDC max). The DUT SiC inverter is voltage controlled. The strategy is an intersected PWM. The modulation reference voltage amplitude (Vmod*) is given with respect to the back-emf gain K = $0.53\sqrt{3}$ V/s of the PMSM. The output of the PWM controller provides the gate duty cycles (d) to the SiC MOSFETs (ga, gb, gc, ga, gb, gc). The switching frequency Fs has been set to 16, 20, and 24 kHz. Duty cycle calculation for the SiC converter, with V_{DC} = 600 V is as follows by Equ. (1):

$$d = \frac{1}{2}.\frac{V_{mod}^{*}}{V_{DC}} + \frac{1}{2} \qquad (1)$$

The tester IGBT/diodes inverter is current controlled. The three phase currents (Ia, Ib, Ic) which represent the PMSM phase currents are controlled using an original modulated hysteresis current controller (HCC), as shown in Fig. 10a), based on the modulated hysteresis method, which is detailed hereafter. The switching frequency F is synchronized with the frequency Fs of the DUT SiC inverter, with a limitation up to Flim ≤ 50 kHz maximum. The output of the modulated hysteresis controller provides the gate duty cycles for the Infineon IGBTs semiconductors (ha, hb, hc, ha, hb, hc). Different load current cycles can be imposed thanks to the IGBT tester, and representative of motor behavior. In the studied flywheel emulator application, the fundamental modulation frequencies are imposed from 200 Hz to 400 Hz, emulating the motor speed (3000 to 6000 rpm). The principle of the testing bench is original; hence it enables the possibility to test all types of DUT inverters, and further to investigate the ageing mechanisms of the semiconductors under specific dynamic PWM constraints.

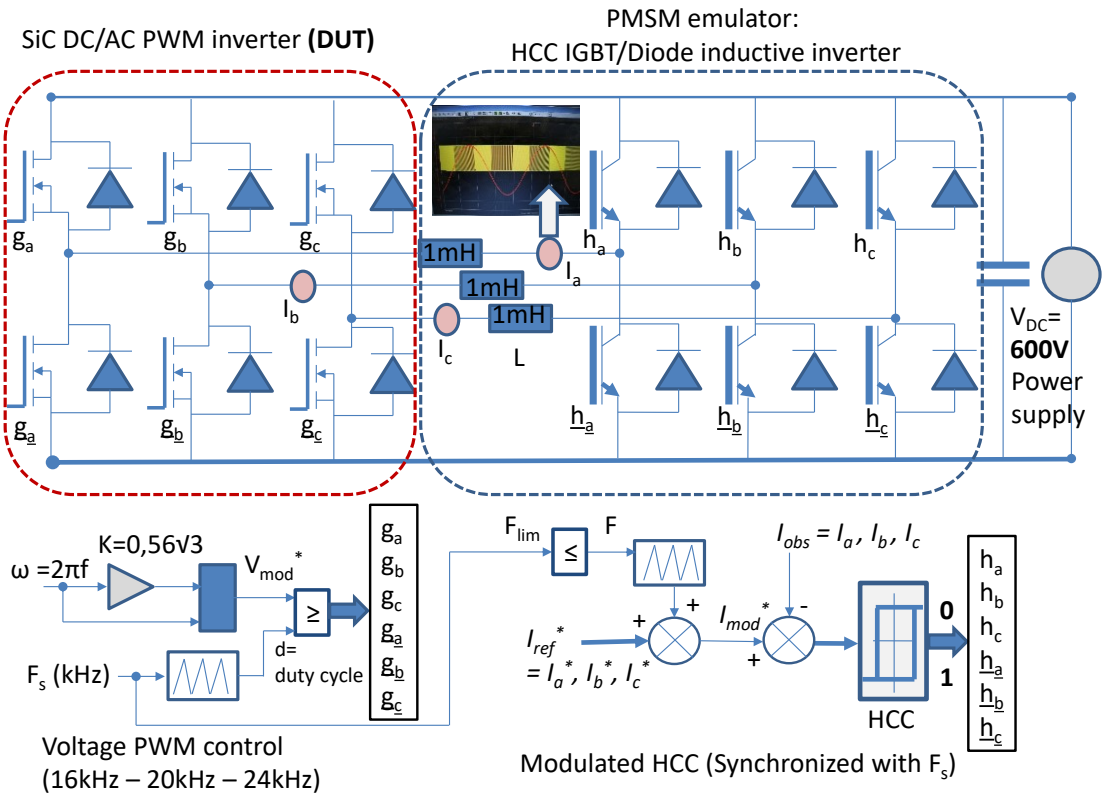

Figure 9. Electrical topology for DC-AC SiC inverter connected to the double-converter architecture

5.2 Original reversible PWM double-converter tester for hardware emulator

In order to control the IGBT/Diode "tester" converter, playing the role of a PMSM emulator, the modulated hysteresis technique has been employed. The principle of this method is detailed and explained in the following paragraph.

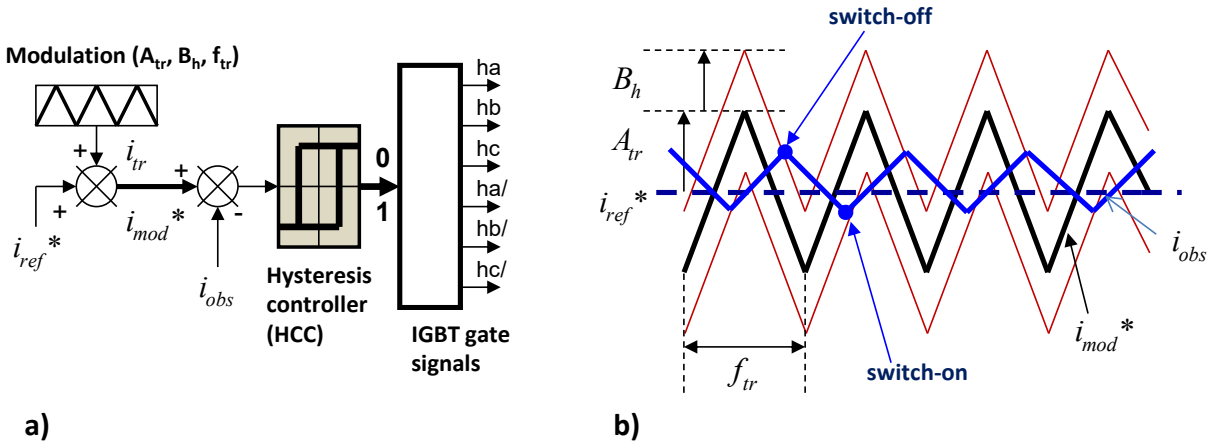

Figure 10. Modulated hysteresis method
a) Hysteresis regulator b) Modulated hysteresis current

An adaptive hysteresis-band control method where the band is modulated with the system parameters in order to maintain the modulation frequency to be nearly constant is presented by B.K. Bose in [22]. Although the technique is applicable to general AC motor drives and other types of load, the modulated hysteresis method permits to impose the switching frequency of the

IGBTs transistors. The hybrid controller, called "modulated hysteresis" controller, combines in one hand the robustness properties of a hysteresis controller and on the other hand the zero static error of a linear proportional integral (PI) controller. In addition, it allows the fixed frequency operation of the converter. It ensures high dynamic response with a fixed-frequency operation mode, a zero static error, and high robustness properties with respect to system parameters variations as shown in [22].
The principle of the method consists in superimposing to the reference current (iref*) a modulated triangular signal (itr) having adequate amplitude Atr and desired frequency ftr (Fig. 10b). We obtain then a modulated reference current (imod*), which constitutes the new reference for the current control loop as given by Equ. 2.

$$i_{mod}{}^{*} = i_{ref}{}^{*} + i_{tr} \tag{2}$$

A judicious choice for Atr and the hysteresis bandwidth Bh impose the switching frequency of the IGBTs transistors equal to that of the triangular signal one. It should be noted that the chosen switching frequency is a compromise between the current ripple rate and the switching losses. Indeed, a higher switching frequency value increases the switching losses of the transistors impacting negatively the global converter efficiency, and on the contrary, for a given “phase-inductance” value, a too small switching frequency creates an important current ripple, which can cause electrical constraints on the semiconductor switches. The modulated hysteresis method is robust, needs only a few parameters in order to be implemented (DC-link voltage source amplitude, the cyclic inductance of the PMSM machine and the desired switching frequency). Moreover the knowledge of a precise model for the PMSM machine is not necessary.
Results of previous studies concerning the modulated hysteresis method in the motor operating-mode show that the sum (Atr + Bh) should verify inequality (3) in order to impose the switching frequency of the transistors equal to that of the triangular signal one:

$$A_{tr} + B_h \rangle \frac{V_{DC}}{4.L.f_{tr}} \tag{3}$$

When using these parameters, the dynamic of the phase current during the commutations is improved and becomes close to that of the current when the classical hysteresis method is applied. Moreover the modulated hysteresis method has still the advantage of a constant switching frequency for the IGBTs transistors.
Concerning the modulated hysteresis method, M.A. Shamsi Nejad et al. in [22] exposed the modeling and study of this new hybrid current controller. It ensures high dynamic response with a fixed-frequency operation mode, a zero static error, and high robustness properties in regard to system parameters variations. To model the proposed nonlinear current controller, different modeling tools have been developed by the authors. In a first step, a high-frequency average model is proposed. It allows studying the average dynamic properties (bandwidth, time response, and overflow) of the method. To investigate the behavior of the current ripple due to the switching effect, a second model, based on the construction of a 3D bifurcation diagram and the definition of a form function, is established. This model allows studying the nature of the cycle described by the state trajectory and proving that the system operates with a fixed switching frequency. Design rules of the control parameters of this controller are explained and its robustness properties are tested by numerical simulations and validated by experimental tests.
Fig. 11 shows the global testing bench: DC-AC SiC inverter connected to the IGBT/Diode tester, developed at SATIE laboratory.

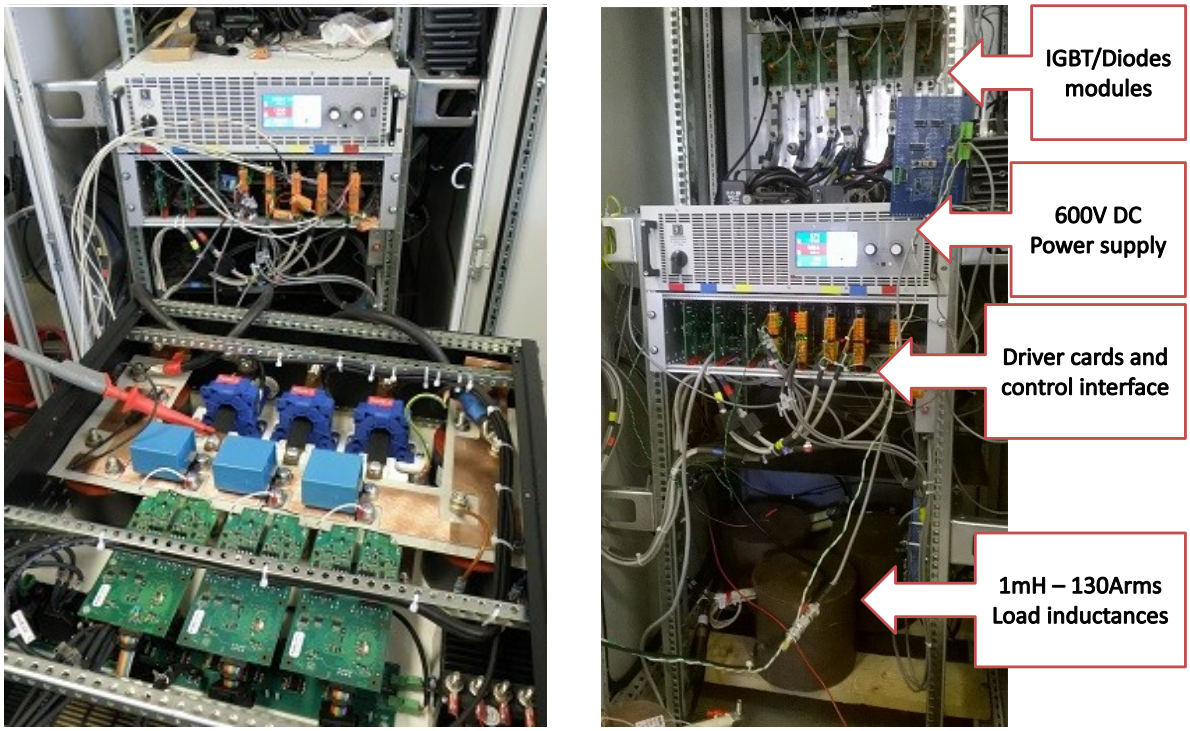

a) SiC converter under test connected to the test bench

b) Test bench with PMSM emulator (IGBT/Diode converter)

Figure 11. Testing bench for SiC prototype inverter testing

5.3 Evaluation of the losses and SiC DC-AC inverter efficiency

The 3-phase DC-AC SiC inverter is water cooled. An appropriated heat-sink has been calculated. Thermal losses P (Watt) are given by the following Equation (4),
Where = 2.9 l/mn is the water cooling flow, Cp the specific heat capacity of water = 4 180 J. kg-1.K-1, and (Two, Twi) resp. the output and input water temperatures.

$$P = \dot{m}_f .C_p .(T_{wo} - T_{wi}) \quad (4)$$

Analytical losses, including copper (Joule) losses and switching losses are deduced from SiC semiconductor datasheets and calculated using formula (5):

$$P = 3.(R_{dsON} .I_{rms}^2 + F_s (E_{on} + E_{off})) \quad (5)$$

Analytically, for 144Arms which is the maximal current constraint, for 24 kHz switching frequency, RdsON=3.5 mΩ at ambient temperature 25°C, RG = 5Ω (external gate resistance present on the driver card), Eon = 5.25 mJ, Eoff= 1.9 mJ, the calculated losses are 732 W which value is in accordance with the losses evolution at 3000 rpm (144A), see results in Fig. 12.
For 20 kHz the losses are 647 W, and for 16 kHz the losses become 561 W.
Efficiencies (in %) are calculated for static points, with Equation 6, for 50 kW transmitted power:

$$E = 100 \times \left(\frac{50000 - P}{50000} \right) \qquad (6)$$

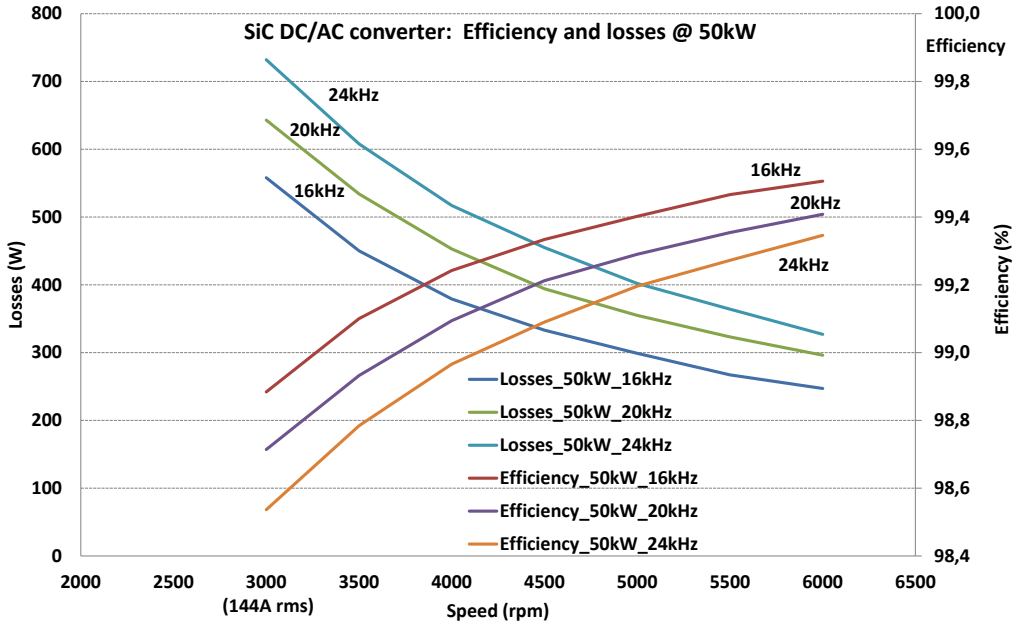

Figure 12. Experimental thermal losses for 50kW test

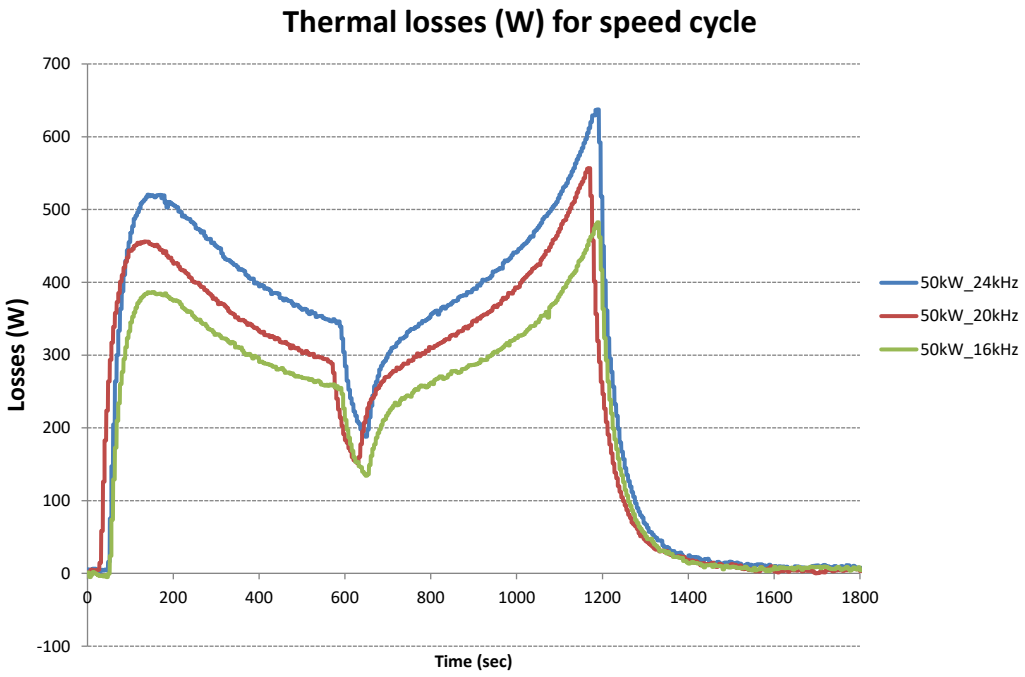

Figure 13. Experimental thermal losses for 50kW speed up and down profile

Efficiencies of the SiC converter (from 16 kHz to 24kHz) are between 99,5% to 99,3%.
Figure 13 represents the thermal losses for a speed up and down cycle from 3000 to 6000 rpm, then from 6000 down to 3000 rpm. The time for current injection is 2 x 9 min = 1080 sec with 1 min pause between the two transients. The average losses for the cycle at 24kHz is 461 W, which deduced efficiency is 99,1 % over the speed up – down cycle.

CONCLUSION

The research work presented in this paper has concerned the design and experimental validation of a 50kW three-phase high efficiency DC-AC inverter with novel Silicon carbide (SiC)-based MOSFETs transistors technology, and used for the supply of an EV-Charging flywheel energy storage system. High frequency switching and PWM tests, and hardware realization have been presented and discussed. The three-phase DC-AC Silicon carbide inverter prototype has been characterized on an original homemade PWM test-bench controlled using a modulated hysteresis controller, and which is able to emulate the working of the motor-flywheel system. Static power tests up to 50kW have been performed, also up-down speed cycle operating and thermal losses have been evaluated. An efficiency above 99% has been reached for the DC-AC three-phase Silicon carbide converter prototype thanks to the adopted design and control strategy. As a further step, the SiC-based inverter prototype should be integrated together with the control master module in order to perform tests over the global motor-flywheel energy storage system, with scenarios representative of EV-charging use cases.

ACKNOWLEDGMENT

Authors gratefully thank the French ministry of Industry, and the Region of Paris Île-de-France, for financing of research within the FUI-13 N° 13021410 grant agreement, and greatest thanks to Dr. Ing. Jean-Pierre Ousten[†], research engineer, for his precious assistance and contribution in the design and realization of the silicon carbide DC-AC reversible inverter prototype.

REFERENCES

1. Riccardo Amirante, Egidio Cassone, Elia Distaso, Paolo Tamburrano, Overview on recent developments in energy storage: Mechanical, electrochemical and hydrogen technologies, *Energy Conversion and Management*, Vol. 132, 15 January 2017, Pages 372-387.
2. A.A. Khodadoost Arani, H. Karami, G.B. Gharehpetian, M.S.A. Hejazi, “Review of Flywheel Energy Storage Systems structures and applications in power systems and microgrids,” *Renewable and Sustainable Energy Reviews*, vol. 69, March 2017, pp. 9-18.
3. S.M. Mousavi G, Faramarz Faraji, Abbas Majazi, Kamal Al-Haddad, “A comprehensive review of Flywheel Energy Storage System technology,” *Renewable and Sustainable Energy Reviews*, vol. 67, January 2017, pp. 477-490.
4. K. Kato, S. Ishiguma, Y. Ito, Y. Ohnuma and S. Miyawaki, "Loss evaluation of matrix converters using SiC-MOSFETs for flywheel energy storage systems," 2015 *IEEE International Telecommunications Energy Conference* (INTELEC), 2015, pp. 1-6, doi: 10.1109/INTLEC.2015.7572484.
5. Koji Kato, Youichi Ito, Satoru Ishiguma, Tsuyoshi Nagano, Kazuhiro Koiwa, Jun-ichi Itoh, “Ultra Long Lifetime Energy Storage System using Flywheels and Matrix Converters,” in *PCIM Europe 2015*; *International Exhibition and Conference for Power Electronics, Intelligent Motion, Renewable Energy and Energy Managemen*t (2015).
6. A. Guettafi and G. Quichaud, Modelling and simulation of an association magnet-multifilamentaries superconductors as spherical bearing for an inertial flywheel with high speed, *Eur. Phys. J. Appl. Phys.* 33, 9-13 (2006).
7. Wang, W., Li, Y., Shi, M., & Song, Y. (2021). Optimization and control of battery-flywheel compound energy storage system during an electric vehicle braking. *Energy*, 226, 120404.
8. L.Barelli, G.Bidini, D.Pelosi, D.A.Ciupageanu, E.Cardelli, S.Castellini, G.Lăzăroiu, Comparative analysis of AC and DC bus configurations for flywheel-battery HESS integration in residential micro-grids, *Energy*, Vol. 204, 1 August 2020, 117939.

9. T. Ben Salah, Y. Lahbib and H. Morel, Modelling, analysis, and experimental study of SiC JFET body diode, *Eur. Phys. J. Appl. Phys*. 53, 10301 (2011).
10. Salinamakki Ramabhatta Gurumurthy, Vivek Agarwal, Archana Sharma, "High-Efficiency Bidirectional Converter for Flywheel Energy Storage Application," *IEEE Transactions on Industrial Electronics* (2016), Vol. 63, n° 9, pp. 5477 – 5487.
11. S.J. Amodeo, H.G. Chiacchiarini, J.A. Solsona, C.A. Busada, High-performance sensorless nonlinear power control of a flywheel energy storage system, *Energy Conversion and Management*, Vol. 50, Issue 7, July 2009, Pages 1722-1729.
12. Salinamakki Ramabhatta Gurumurthy, Vivek Agarwal, Archana Sharma, A Novel Dual-Winding BLDC Generator–Buck Converter Combination for Enhancement of the Harvested Energy From a Flywheel, *IEEE Transactions on Industrial Electronics*, Year: 2016, Vol. 63, Issue: 12, Pages: 7563 – 7573.
13. Koos van Berkel, Sander Rullens, Theo Hofman, Bas Vroemen, Maarten Steinbuch, Topology and Flywheel Size Optimization for Mechanical Hybrid Powertrains, *IEEE Transactions on Vehicular Technology*, (2014), Vol.: 63, Issue: 9, Pages: 4192 – 4205.
14. M. A. H. Rafi and J. Bauman, "A Comprehensive Review of DC Fast-Charging Stations With Energy Storage: Architectures, Power Converters, and Analysis," in *IEEE Transactions on Transportation Electrification*, vol. 7, no. 2, pp. 345-368, June 2021.
15. Bo Sun, Tomislav Dragičević, Francisco D. Freijedo, Juan C. Vasquez, Josep M. Guerrero, A Control Algorithm for Electric Vehicle Fast Charging Stations Equipped With Flywheel Energy Storage Systems, *IEEE Transactions on Power Electronics*, (2016), Vol. 31, Issue: 9, Pages: 6674 – 6685.
16. Jukkrit Noppakunkajorn, Di Han, Bulent Sarlioglu, Analysis of High-Speed PCB With SiC Devices by Investigating Turn-Off Overvoltage and Interconnection Inductance Influence, *IEEE Transactions on Transportation Electrification*, (2015), Vol.: 1, Issue: 2, Pages: 118 – 125.
17. N. F. Ershad, R. T. Mehrjardi and M. Ehsani, "Development of a Kinetic Energy Recovery System Using an Active Electromagnetic Slip Coupling," in *IEEE Transactions on Transportation Electrification*, vol. 5, no. 2, pp. 456-464, June 2019.
18. Xiaolin Tang, Xiaosong Hu, Wei Yang, Haisheng Yu, Novel Torsional Vibration Modeling and Assessment of a Power-Split Hybrid Electric Vehicle Equipped With a Dual-Mass Flywheel, *IEEE Transactions on Vehicular Technology*, Year: 2018 , Volume: 67 , Issue: 3, Pages: 1990 – 2000.
19. K. Itani, A. De Bernardinis, Z. Khatir, A. Jammal, Comparative analysis of two hybrid energy storage systems used in a two front wheel driven electric vehicle during extreme start-up and regenerative braking operations, *Energy Conversion and Management*, Vol. 144, 15 July 2017, Pages 69-87.
20. A. De Bernardinis, A. Kolli, J.-P. Ousten, R. Lallemand, High efficiency Silicon carbide DC-AC inverter for EV-charging Flywheel system, 2017 *IEEE Transportation Electrification Conference and Expo (ITEC)*, 2017, Pages: 421 – 424.
21. Kolli, A., De-Bernardinis, A., Khatir, Z., Gaillard, A., Béthoux, O., & Hissel, D. (2015, November). Part-load control stategy of a 20kW SiC power converter for embedded PEMFC multi-stack architectures. In *IECON* 2015-41st Annual Conference of the IEEE Industrial Electronics Society (pp. 004627-004632). IEEE.
22. B.K. Bose, An adaptive hysteresis-band current control technique of a voltage-fed PWM inverter for machine drive system, Industrial Electronics, IEEE Transactions on 37 (5) (1990) 402 – 408. M. Ali-Shamsi Nejad, S. Pierfederici, J.-P. Martin, F. Meibody-Tabar, Study of an Hybrid Current Controller Suitable for DC–DC or DC–AC Applications, *IEEE Transactions on Power Electronics*, Vol.: 22, Issue: 6, Nov. 2007, Page(s): 2176 – 2186.